A New Technique for Tracking the Global Maximum Power Point of PV Arrays Operating Under Partial-Shading Conditions

Eftichios Koutroulis, *Member, IEEE*, and Frede Blaabjerg, *Fellow, IEEE*

***Abstract*—The power–voltage characteristic of photovoltaic (PV) arrays operating under partial-shading conditions exhibits multiple local maximum power points (MPPs). In this paper, a new method to track the global MPP is presented, which is based on controlling a dc/dc converter connected at the PV array output, such that it behaves as a constant input-power load. The proposed method has the advantage that it can be applied in either stand-alone or grid-connected PV systems comprising PV arrays with unknown electrical characteristics and does not require knowledge about the PV modules configuration within the PV array. The experimental results verify that the proposed global MPP method guarantees convergence to the global MPP under any partial-shading conditions. Compared with past-proposed methods, the global MPP tracking process is accomplished after far fewer PV array power perturbation steps.**

***Index Terms*—DC–DC power converters, maximum power point tracking (MPPT), microcontrollers, photovoltaic (PV) systems.**

I. Introduction

IN TYPICAL photovoltaic (PV) installations, PV arrays are formed by connecting multiple PV modules in various configurations (i.e., series, parallel, series–parallel, etc.) [1]. A bypass diode [2] or bypass switch [3] is connected in parallel with each PV module to protect the solar cells against efficiency degradation and hot-spot failure effects. Under uniform solar irradiation conditions among the individual PV modules, the power–voltage (*P–V*) characteristic of the PV array exhibits a unique operating point where the PV generated power is maximized (maximum power point, MPP). Many MPP tracking (MPPT) methods have been developed in the past in order to operate the PV array at the MPP point [4], enabling the maximization of the PV energy production under the continuously changing solar irradiation and ambient temperature conditions.

However, in the case in which one or more of the PV modules comprising the PV array are shaded (e.g., due to dust, shading from surrounding buildings, trees or poles, nonuniform solar irradiation incidence on contoured flexible PV arrays [5] in portable and building integrated PV applications, etc.), then the *P–V* characteristic of the PV array exhibits multiple local maxima and only one of them corresponds to the global MPP. Examples of the *P–V* characteristics of a PV array operating under uniform and nonuniform solar irradiation conditions are depicted in Fig. 1. The PV array output power at the global MPP is lower than the sum of the maximum available power levels that the individual PV modules are able to provide [6]. As analyzed in [7], under practical operating conditions, the location and magnitude of the local and global MPPs depend on the stochastically varying shading pattern area and geometry, as well as the configuration of the PV modules within the PV array.

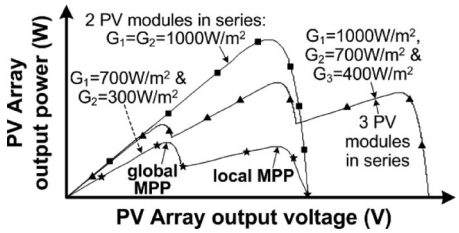

Fig. 1. Examples of the *P–V* characteristics of a PV array composed of identical series-connected PV modules with bypass diodes for different irradiations.

The connection of PV cells and modules in parallel, which is proposed in [8] in order to avoid the effect of partial shading, is applicable only in low-power PV systems (e.g., for portable applications). Using the distributed MPPT (DMPPT) technique, a dc/dc power converter with MPPT controller is incorporated at each PV module of the PV array [6], [9], thus increasing the total available MPP power of the PV array. However, the entire PV array is usually connected to a central power electronic converter in order to reduce the PV system cost and implementation complexity [1].

Under partial-shading conditions, the conventional MPPT techniques fail to guarantee successful tracking of the global MPP [10], resulting in significant reduction of both the generated power and the PV energy production system reliability [11]. According to measurements performed under real operating conditions of PV systems, the power loss due to the MPPT algorithm convergence to a local (instead of the global) MPP may be up to 70% [11]. In the "1000 rooftop PV systems" program implemented in Germany, it has been recorded that the operation of the 41% of the installed PV systems had been affected by shading, with energy losses of the order of 10% [12].

The reconfiguration of the connections between the individual PV modules comprising the PV array, using a matrix of power

Manuscript received August 19, 2011; revised December 23, 2011; accepted January 3, 2011. Date of publication February 7, 2012; date of current version March 16, 2012.

E. Koutroulis is with the Department of Electronic and Computer Engineering, Technical University of Crete, Chania GR-73100, Greece (e-mail: efkout@electronics.tuc.gr).

F. Blaabjerg is with the Department of Energy Technology, Aalborg University, Aalborg DK-9220, Denmark (e-mail: fbl@et.aau.dk).

Digital Object Identifier 10.1109/JPHOTOV.2012.2183578

switches, has been proposed in [13]. The target of this reconfiguration is to form the parallel-connected strings comprising the PV array such that they consist of PV modules operating under similar solar irradiation conditions. Using this method, both the PV energy production system complexity and cost are significantly increased.

The application of the global MPPT algorithm that is proposed in [14] requires the characterization of the PV source after each partial-shading topology has been established. In [15], the equations for the calculation of the local MPPs of partially shaded multicrystalline silicon PV modules are provided. In [16], the global MPP is tracked by scanning the *P–V* curve based on information of the PV modules open-circuit voltage and their configuration on the PV array. The global MPPT methods that are presented in [17] and [18] are based on the measurements of the PV array open-circuit voltage and solar irradiation or short-circuit current, respectively. The sequential extremum seeking control algorithm and the incremental conductance-based MPPT method with step-size variation are applied in [19] and [20], respectively. A common drawback of these methods is that they require knowledge of the electrical characteristics of the PV modules and/or their configuration within the PV array. Thus, they are not really applicable for the development of commercial PV power processing interfaces, where both the PV array configuration and the PV modules electrical characteristics applied by the end user are generally unknown. Additionally, the accuracy of the calculations is affected by the PV modules' electrical parameters deviation due to aging. The use of specialized sensors (e.g., for the measurement of solar irradiation) increases the PV system cost, while on the other hand, during the measurement of the PV array open-circuit voltage or short-circuit current, the PV energy production is suspended.

In [21], a radial basis function and a three-layered feed-forward neural network are used to track the global MPP, having the disadvantage that the MPPT control system implementation complexity is highly increased. Additionally, considerable computational efforts are required during the neural network training in order to ensure that the global MPPT process will be performed reliably and accurately under any shading conditions.

The MPPT algorithm that is based on a Fibonacci sequence [22] does not guarantee convergence to the global MPP. The particle swarm optimization (PSO) [23], genetic algorithms [24], and differential evolution (DE) [25] global MPPT approaches, and the stochastic algorithm based on the chaos search theory, which is presented in [26], exhibit significant algorithmic complexity, which increases the implementation cost of the global MPPT control system.

The detection of local MPPs using a periodic scan sequence of the *P–V* curve is frequently employed in commercially available PV power conditioning devices [27]. Due to the long time required for the completion of this process, the PV energy production is reduced. A global MPPT scheme that is based on the dividing rectangles optimization algorithm is proposed in [28], having the advantage of avoiding the computation of the *P–V* function gradient. However, it is not guaranteed that, under any partial-shading conditions, the convergence to the global MPP will be achieved in fewer steps than an exhaustive search procedure scanning the entire *P–V* curve.

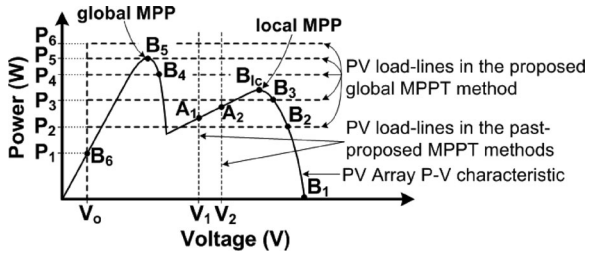

Fig. 2. Operating principles of global MPPT methods.

The algorithmic complexity and tracking inefficiency of the methods described previously arise because these methods are based on searching for the global MPP by iteratively controlling the operating voltage of the PV array load according to the corresponding MPPT algorithm. As illustrated in Fig. 2, the resulting operating point of the PV array lies on the intersection of the PV array and load *P–V* characteristics (e.g., points A_1 and A_2). Thus, the past-proposed algorithms are unable to guarantee the discrimination between local and global MPPs, unless the PV array output power is measured at a large number of operating points, spread over the entire voltage range of the PV array.

In this paper, a new method to track the global MPP of PV arrays operating under partial-shading conditions, in either stand-alone or grid-connected PV systems, is presented. The PV array is connected to a dc/dc power converter, which is controlled by a microcontroller-based control unit. Initially, the power converter is controlled to operate as an adjustable constant input-power load. With reference to the *P–V* characteristics depicted in Fig. 2, starting from the PV array open-circuit condition (point B_l), the dc/dc converter is controlled to draw a successively higher amount of power. Hence, the PV array operating point is progressively moved toward higher output power levels (points B_1, B_2, B_3, B_4, and B_5). It is observed that using this process, the proposed algorithm avoids getting trapped in the local MPP (point B_{lc} in Fig. 2) and successfully detects the existence of the PV array operating points B_4 and B_5, which provide higher output power compared with the local MPP, without performing a *P–V*-curve scanning procedure over a wide voltage range. This process is continued until convergence to point B_6 is detected, where the PV array output power increment is inhibited. This condition indicates that the previous PV array operating point (i.e., B_5 in Fig. 2) provides the maximum possible PV array output power, thus corresponding to the global MPP. Then, the dc/dc converter is controlled such that the PV array output voltage is regulated to the global MPP point B_5 detected in the previous phase of the algorithm. The experimental results that are presented in this paper verify that using this method enables the successful detection of the global MPP, irrespective of the number of local MPPs exhibited by the PV array *P–V* characteristic and their location relative to the global MPP. The global MPPT detection procedure described previously is executed periodically (e.g., every 1–15 min). Then, the perturb and observe (P&O) MPPT process is applied in order to continuously

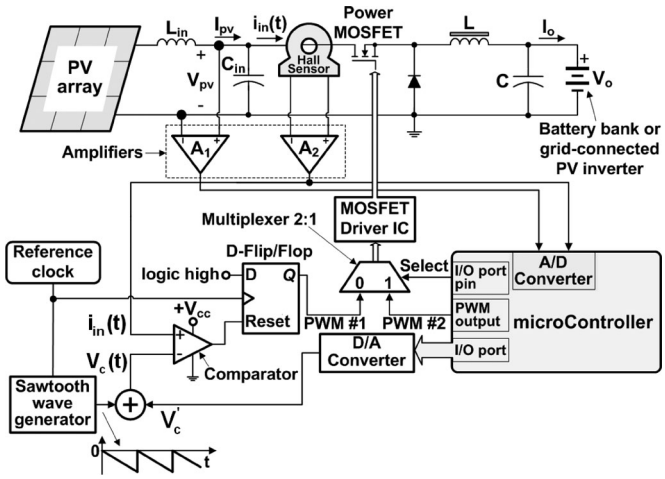

Fig. 3. Detailed block diagram of the proposed global MPPT system.

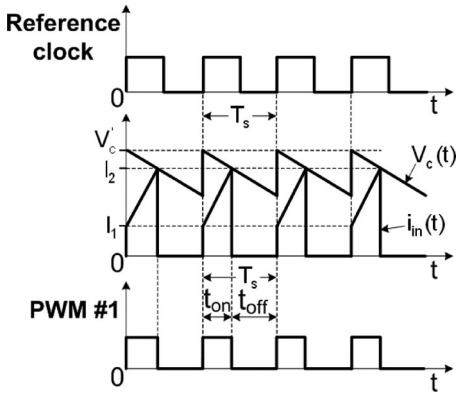

Fig. 4. Principal waveforms of the proposed global MPPT system.

track the short-term variations of the previously detected global MPP. According to [27], the iterative application of a *P–V*-curve scan sequence, with a 15-min scan interval, results in a less than 0.06% maximum energy loss on unshaded arrays. As it will be demonstrated in the experimental results, the proposed global MPPT process is less time consuming than the *P–V*-curve scanning method. Thus, the periodic execution of the proposed global MPPT process does not result in significant energy loss in the case that the PV array is actually unshaded. The P&O MPPT algorithm has been selected because of its implementation simplicity, flexibility, and robustness [29]. However, any of the past-proposed MPPT algorithms [4] can also be applied in order to conform with specific PV system design specifications. Compared with the past-proposed global MPPT techniques, the method that is presented in this paper has the advantage that it does not require knowledge of the electrical characteristics of the PV modules and their configuration within the PV array. In the following sections of this paper, the proposed global MPPT system is first analyzed in detail and then validated by experimental results.

II. Proposed Global Maximum Power Point Tracking System

A detailed diagram of the proposed global MPPT system is depicted in Fig. 3. Depending on the PV system application domain, a buck-type dc/dc power converter is used to interface the PV array output power to either a battery bank or a dc/ac inverter connected to the electric grid [30], [31]. Both of these alternative types of dc/dc converter load are represented in Fig. 3 by the voltage source V_o. The inductance of the cable connecting the PV array to the dc/dc converter $L_{\rm in}$ is considered for stability analysis purposes, as discussed in the following. The inductor L and the input and output filter capacitor values $C_{\rm in}$ and C, respectively, are calculated as described in [32] such that the dc/dc converter operates in continuous conduction mode, and simultaneously, the input and output voltage ripple factors are reduced to an acceptable limit. The PV array voltage is measured using an operational amplifier-based differential amplifier, and the dc/dc converter input current is measured with a Hall-effect-based current sensor. The proposed global MPPT procedure is performed in three consecutive phases: the constant input power, PV array voltage regulation, and P&O stage. In order to execute these processes, the dc/dc power converter is controlled using either the "PWM #1" or the "PWM #2" control signals depicted in Fig. 3, which are produced as analyzed in the following.

A. DC/DC Converter Constant Input-Power Mode

In this section, the dc/dc converter operation and control, such that it behaves as an adjustable constant input-power load, is presented. The operation of the dc/dc converter in this operating mode constitutes the basis for the detection of the PV array global MPP, according to the proposed global MPPT control algorithm.

The input–output voltage relationship of a buck-type dc/dc converter is the following:

$$V_o = D \cdot V_{\rm pv} = \frac{t_{\rm on}}{T_s} \cdot V_{\rm pv} \tag{1}$$

where $V_{\rm pv}$ and V_o (in volts) are the dc/dc converter input and output voltage levels, respectively, D is the converter duty cycle ($0 \leq D \leq 1$), T_s is the switching period, and $t_{\rm on}$ is the ON time of the power MOSFET pulsewidth modulation (PWM) control signal.

The "PWM #1" control signal, which is depicted in Fig. 3, is produced by comparing the instantaneous value of the dc/dc converter input current $i_{\rm in}(t)$ with the control signal $V_c(t)$ generated by the control unit. The corresponding waveforms are plotted in Fig. 4. The average value of $i_{\rm in}(t)$ is equal to the PV array dc output current $I_{\rm pv}$ (in ampere), and it is given by

$$\begin{aligned} I_{\rm pv} &= \frac{1}{T_s} \cdot \int_0^{t_{\rm on}} \left(I_1 + \frac{V_{\rm pv} - V_o}{L} t \right) dt \\ &= \frac{1}{T_s} I_1 t_{\rm on} + \frac{1}{T_s} \cdot \frac{V_{\rm pv} - V_o}{L} \cdot \frac{t_{\rm on}^2}{2}. \end{aligned} \tag{2}$$

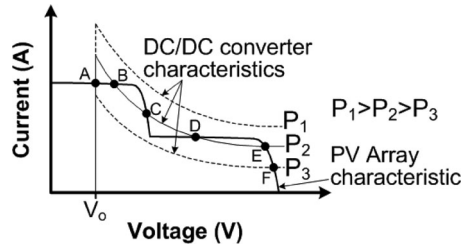

Fig. 5. Current–voltage characteristics of the PV array and the dc/dc converter operating under partial-shading and constant-input-power conditions, respectively.

Since $i_{\rm in}(t_{\rm on}) = V_c(t_{\rm on})$, the value of I_1 in (2) is calculated using (1), as follows:

$$I_1 + \frac{V_{\rm pv} - V_o}{L} t_{\rm on} = I_1 + \frac{V_o}{L}(T_s - t_{\rm on}) = V_c(t_{\rm on}) = I_2$$

$$\Rightarrow I_1 = V_c(t_{\rm on}) - \frac{V_o}{L}(T_s - t_{\rm on}). \quad (3)$$

Combining (2) and (3), the dc/dc converter average input power $P_{\rm pv}$ (in Watts) is calculated using the following equation:

$$P_{\rm pv} = V_{\rm pv} I_{\rm pv} = V_c(t_{\rm on}) V_o - \frac{V_o^2 T_s}{2L} + \frac{V_o^2 t_{\rm on}}{2L}. \quad (4)$$

In the proposed method, the values of $V_c(t)$ and V_c' are selected such that $V_c(t) = V_c' - (V_o/2L)t$, thus resulting in

$$P_{\rm pv} = V_c' V_o - \frac{V_o^2 T_s}{2L} \quad (5)$$

where V_c' is a dc control signal of adjustable amplitude, produced by the control unit according to the global MPPT algorithm analyzed in the next section.

The dc/dc converter output voltage V_o depends on either the slowly changing battery state of charge (in stand-alone applications) or the electric-grid voltage (in grid-connected PV systems) and remains approximately constant during the consecutive steps of the global MPPT process. Since the values of T_s and L are also constant, it is concluded from (1) and (5) that, for $V_{\rm pv} \geq V_o$, the dc/dc converter input power can be regulated to the desired level by adjusting the amplitude of the V_c' control signal (constant input-power mode of operation).

The current–voltage characteristics of the PV array and dc/dc converter operating under partial-shading and constant-input-power conditions, respectively, are depicted in Fig. 5. The points of intersection (i.e., points A, B, C, etc., in Fig. 5) define the equilibrium operating points of the interconnected PV array-dc/dc converter system. Practically, the cable inductance $L_{\rm in}$ is negligible. Thus, according to the stability analysis that is presented in [33], which has been performed for a PV array connected to a constant power load (e.g., a switching power converter with regulated output voltage) in a spacecraft power processing system, the points A, C, E, and F in Fig. 5 are stable, while points B and D are unstable. The points A, C, E, and F in Fig. 5 correspond to the points B_l–B_6 and B_{lc} of the *P–V* curve depicted in Fig. 2. In the proposed method, the global MPP is tracked by controlling the dc/dc converter such that it behaves as a constant input-power load, and simultaneously, the PV array operates at the stable operating points A, C, E, and F, according to the algorithm analyzed next.

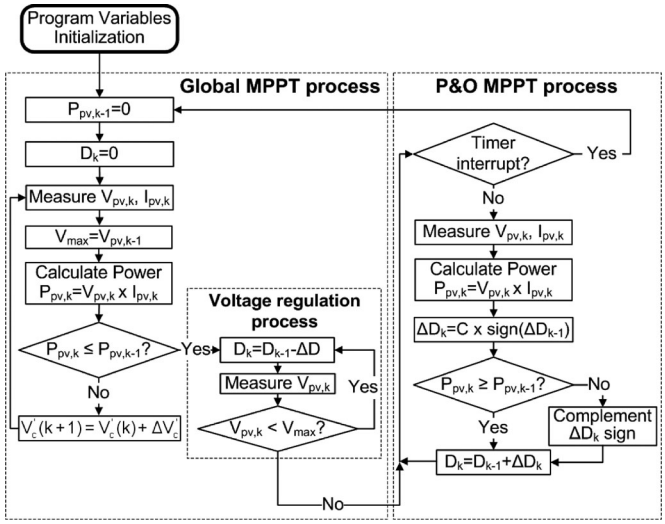

Fig. 6. Flowchart of the proposed global MPPT control algorithm.

B. Global Maximum Power Point Tracking Algorithm

A flowchart of the proposed global MPPT control algorithm is shown in Fig. 6. Initially, the global MPPT process is performed in order to detect the position of the global MPP of the PV array. During that phase of the proposed algorithm, the power converter control method is set such that the power converter operates as an adjustable constant input-power load, as analyzed in the previous section. The power drawn by the dc/dc converter (i.e., the PV array output power) is iteratively increased by appropriately adjusting the amplitude of the V_c' control signal output by the D/A converter, as follows:

$$V_c'(k) = V_c'(k-1) + \Delta V_c' \quad (6)$$

where $V_c'(k)$ and $V_c'(k-1)$ are the V_c' signal values at steps k and $k-1$, respectively (initially $V_c'(0) = 0$), and $\Delta V_c'$ is the constant perturbation applied.

Increasing the value of $\Delta V_c'$ in (6) results not only in a reduction of the time required to detect the PV array global MPP, but also reduce the ability of the algorithm to discriminate local and global MPPs of similar power levels.

At each step, the PV array operating voltage is measured and stored in the microcontroller memory. This process is repeated until the operating point of the interconnected PV array dc/dc converter system moves to point B_6 depicted in Fig. 2, where the PV array output power increment is inhibited. This condition indicates that the PV array output power measured during the previous step of the algorithm corresponds to the global MPP. Then, the dc/dc converter duty cycle is iteratively reduced until the PV array output voltage is regulated to the global MPP. Only the PV array output voltage is measured in order to perform this process. The procedure presented previously is applied periodically (e.g., 1–15 min) to detect the position of the global MPP of the PV array. Then, the P&O MPPT algorithm is executed in order to maintain operation at the previously detected global

MPP during the short-term variations of solar irradiation and ambient temperature conditions.

During the P&O MPPT process, the dc/dc converter average input power is calculated by measuring the PV array output voltage and current. The resulting value is compared with the input power measured during the previous iteration of the algorithm. According to the result of the comparison, the duty cycle of the "PWM #2" dc/dc converter PWM control signal, which is depicted in Fig. 3, is modified as follows:

$$D_k = D_{k-1} + \Delta D_k$$
$$\Delta D_k = C \cdot \text{sign}\left(\Delta D_{k-1}\right) \cdot \text{sign}(P_{\text{pv},k} - P_{\text{pv},k-1}) \quad (7)$$

where ΔD_k is the duty cycle change at step k; $P_{\text{pv},k}$ and $P_{\text{pv},k-1}$ are the PV array output power levels at steps k and $k-1$, respectively, C; is a constant determining the speed and accuracy of convergence to the MPP point; and the function $\text{sign}(x)$ is defined as

$$\text{sign}(x) = 1, \quad \text{if } x \geq 0$$
$$\text{sign}(x) = -1, \quad \text{if } x < 0. \quad (8)$$

The duty cycle is changed continuously according to the P&O algorithm, resulting in steady-state operation around the global MPP. A method for the optimal selection of the parameter C in (7) is described in [29].

III. Experimental Results

A laboratory-prototype global MPPT system operating according to the proposed methodology has been developed and tested under outdoor conditions. The control unit of the proposed global MPPT system, which is illustrated in Fig. 3, has been built around the Atmel AVR ATMEGA8535 microcontroller, which features a 10-bit, eight-channel, A/D converter and on-chip 8-bit PWM outputs. The switching frequency of the "PWM #2" control signal has been set to 31.25 kHz. The PV array which has been used consists of three PV modules connected in series with a bypass diode in parallel with each module. The MPP power and voltage ratings of each PV module under standard test conditions are 5 W and 17.82 V, respectively. For performance validation purposes, a buck-type power converter output has been connected to a 12-V, 7-Ah lead-acid battery. In addition, the PV modules comprising the PV array were installed at different tilt angles such that they receive unequal amounts of solar irradiation. Thus, the resulting *P–V* characteristic of the PV array exhibits both local and global MPPs.

Initially, the PV modules were installed such that the global MPP is located at a higher voltage compared with the local MPPs (test case #1). The corresponding *P–V* characteristic of the PV array was experimentally measured using a *P–V*-curve scan process, and it is plotted in Fig. 7(a). Then, the proposed global MPPT method was applied. The experimentally measured operating points of the PV array during the execution of the proposed global MPPT process (i.e., points P_1–P_{12}) are also indicated in Fig. 7(a). The minimum possible operating voltage of the PV array is 11 V, since a discharged battery has been connected at the dc/dc converter output terminals. The global MPP

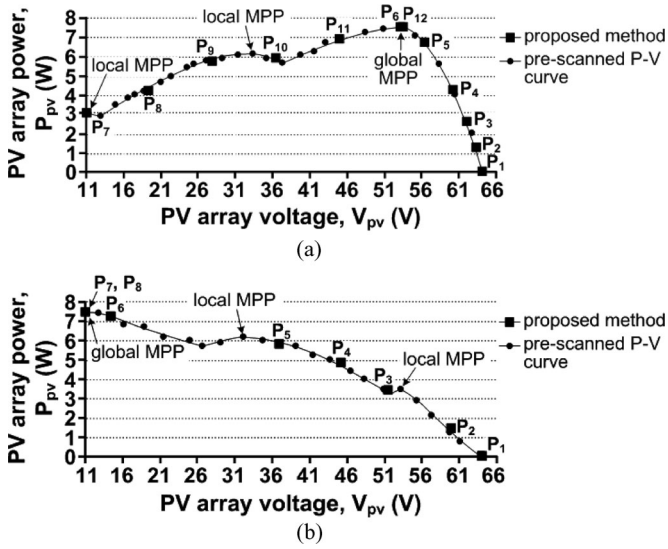

Fig. 7. Experimentally measured *P–V* characteristic of the PV array and the PV array operating points during the operation of the proposed global MPPT system in the case in which the global MPP is located at (a) higher voltage (test case #1) and (b) lower voltage (test case #2), compared with the local MPPs.

detection process was initiated, setting the PV array under an open-circuit operating condition (point P_1). By progressively increasing the value of the control signal V_c', the dc/dc converter was controlled such that it draws an increasing amount of power, thus causing the successive movement of the PV array operating points in the trajectory $P_1 \rightarrow P_2 \rightarrow P_3 \rightarrow P_4 \rightarrow P_5 \rightarrow P_6$. At point P_6, the next increment of the dc/dc converter input power moved the PV array operating point at P_7 (11 V, 3.03 W). The resulting reduction of the PV array output power was sensed by the microcontroller-based control unit, provoking the dc/dc converter operation in the voltage regulation mode. Thus, the dc/dc converter PWM control signal duty cycle was iteratively reduced until the PV array operating point was restored at point P_{12} (52.9 V, 7.44 W), where the highest PV output power was measured during the previous phase of the algorithm through the trajectory $P_7 \rightarrow P_8 \rightarrow P_9 \rightarrow P_{10} \rightarrow P_{11} \rightarrow P_{12}$. Then, the execution of the P&O MPPT algorithm was initiated, resulting in a continuous oscillation of the PV array operating point around the previously detected global MPP (i.e., point P_{12}). During the P&O MPPT process, the maximum deviation of the PV array operating power from the global MPP has been experimentally measured to be equal to 0.43%.

In order to validate that the proposed global MPPT method is equally efficient, irrespective of the relative position of the local and global MPPs, the PV modules were also installed such that the global MPP is located at a lower voltage compared with the local MPPs (test case #2). The resulting P–V characteristic of the PV array was experimentally measured using a *P–V*-curve scan process, and it is illustrated in Fig. 7(b). Then, the proposed global MPPT algorithm was executed. The experimentally measured operating points of the PV array during the execution of the proposed global MPPT process (i.e., points P_1–P_8) are also depicted in Fig. 7(b). During the global MPP detection phase of the proposed algorithm, the PV array operating

TABLE I
EXPERIMENTALLY MEASURED NUMBER OF PV ARRAY POWER PERTURBATION STEPS REQUIRED TO DERIVE THE GLOBAL MPP

	Proposed algorithm	PV-curve scan	Particle Swarm Optimization (PSO)	Differential Evolution (DE)
Test case #1	12	50	33	2020
Test case #2	8	50	27	2020

point is continuously displaced, following the sequence $P_1 \rightarrow P_2 \rightarrow P_3 \rightarrow P_4 \rightarrow P_5 \rightarrow P_6 \rightarrow P_7$. In the test case that is presented in Fig. 7(b), the global MPP is located at the minimum possible operating voltage of the PV array (i.e., 11 V). Thus, at P_7 (11 V, 7.45 W), the next increment of the V_c' control signal does not alter the PV array operating conditions, indicating that the resulting point P_8 (11 V, 7.45 W) is the global MPP. During the voltage-regulation mode initiated next, the PV array operating point was held at the global MPP point detected at the previous step (i.e., point P_8). Then, the P&O MPPT process was performed in order to track the short-term variations of the global MPP. Due to the oscillations inherent in the P&O MPPT process, the maximum deviation of the PV array operating power from the global MPP in this test case has been experimentally measured to be equal to 0.08%.

In both of the test cases analyzed previously, the proposed global MPPT algorithm successfully avoided getting trapped in local optima and achieved convergence to the global MPP of the PV array. The microcontroller-based control unit of the laboratory-prototype global MPPT system was also programmed to track the PV array global MPP in the two test cases described previously according to the *P–V*-curve scan sequence [27], PSO [23], and DE [25] methods. Only the "PWM #2" control signal (see Fig. 3) has been used for that purpose. In the *P–V*-curve scan sequence algorithm, the duty-cycle perturbation step has been set equal to that of the proposed algorithm [see parameter C in (7)]. The values of the parameters affecting the operation of the PSO and DE algorithms (e.g., number of agents in the PSO method, termination criterion, etc.) have been set as described in [23] and [25], respectively. All algorithms successfully detected the position of the global MPP. The experimentally measured numbers of the PV array power perturbation steps required by each algorithm in order to derive the global MPP are given in Table I. It is observed that compared with past-proposed methods, using the algorithm presented will result in a much faster convergence to the global MPP.

IV. CONCLUSION

The detection of global MPP is indispensable in order to maximize the PV system energy production in the case of PV array partial shading. In this paper, a new method has been presented to track the global MPP of PV arrays in either stand-alone or grid-connected PV systems, which is based on controlling the dc/dc power converter connected at the PV array output such that it behaves as a constant input-power load. Compared with the past-proposed global MPPT techniques, the method proposed in this paper has the advantage that it can be applied in PV arrays with unknown electrical characteristics and does not require knowledge of the PV modules configuration within the PV array. The experimental results verify that the proposed method guarantees convergence to the global MPP under any partial-shading conditions. Additionally, the global MPPT process is accomplished with significantly less PV array power perturbation steps than those obtained using past-proposed techniques. The proposed method can easily be incorporated into any existing MPPT control system in both high nominal-power-rating PV systems and low-power energy harvesting applications.

ACKNOWLEDGMENT

The first author would like to thank his former graduate student Y. Kalogiannakis for his contribution during the laboratory-prototype construction and experimental measurements.

REFERENCES

[1] H. Ghoddami and A. Yazdani, "A single-stage three-phase photovoltaic system with enhanced maximum power point tracking capability and increased power rating," *IEEE Trans. Power Del.*, vol. 26, no. 2, pp. 1017–1029, Apr. 2011.

[2] S. Dongaonkar, M. A. Alam, Y. Karthik, S. Mahapatra, D. Wang, and M. Frei, "Identification, characterization, and implications of shadow degradation in thin film solar cells," in *Proc. IEEE Int. Rel. Phys. Symp.*, 2011, pp. 5E.4.1–5E.4.5.

[3] G. Acciari, D. Graci, and A. La Scala, "Higher PV module efficiency by a novel CBS bypass," *IEEE Trans. Power Electron.*, vol. 26, no. 5, pp. 1333–1336, May 2011.

[4] B. N. Alajmi, K. H. Ahmed, S. J. Finney, and B. W. Williams, "Fuzzy-logic-control approach of a modified hill-climbing method for maximum power point in microgrid standalone photovoltaic system," *IEEE Trans. Power Electron.*, vol. 26, no. 4, pp. 1022–1030, Apr. 2011.

[5] P. Sharma, B. Patnaik, S. P. Duttagupta, and V. Agarwal, "Dynamic power optimization of contoured flexible PV array under non-uniform illumination conditions," in *Proc. 35th IEEE Photovoltaic Spec. Conf.*, 2010, pp. 968–972.

[6] G. Adinolfi, N. Femia, G. Petrone, G. Spagnuolo, and M. Vitelli, "Energy efficiency effective design of DC/DC converters for DMPPT PV applications," in *Proc. 35th Annu. Conf. IEEE Ind. Electron.*, 2009, pp. 4566–4570.

[7] R. Ramaprabha, B. Mathur, M. Murthy, and S. Madhumitha, "New configuration of solar photovoltaic array to address partial shaded conditions," in *Proc. 3rd Int. Conf. Emerging Trends Eng. Technol.*, 2010, pp. 328–333.

[8] L. Gao, R. A. Dougal, S. Liu, and A. Iotova, "Parallel-connected solar PV system to address partial and rapidly fluctuating shadow conditions," *IEEE Trans. Ind. Electron.*, vol. 56, no. 5, pp. 1548–1556, May 2009.

[9] S. Poshtkouhi and O. Trescases, "Multi-input single-inductor dc–dc converter for MPPT in parallel-connected photovoltaic applications," in *Proc. 26th Annu. IEEE Appl. Power Electron. Conf. Expo.*, 2011, pp. 41–47.

[10] E. Karatepe, Syafaruddin, and T. Hiyama, "Simple and high-efficiency photovoltaic system under non-uniform operating conditions," *IET Renewable Power Generat.*, vol. 4, no. 4, pp. 354–368, 2010.

[11] G. Petrone, G. Spagnuolo, R. Teodorescu, M. Veerachary, and M. Vitelli, "Reliability issues in photovoltaic power processing systems," *IEEE Trans. Ind. Electron.*, vol. 55, no. 7, pp. 2569–2580, Jul. 2008.

[12] M. Drif, P. J. Perez, J. Aguilera, and J. D. Aguilar, "A new estimation method of irradiance on a partially shaded PV generator in grid-connected photovoltaic systems," *Renewable Energy*, vol. 33, pp. 2048–2056, 2008.

[13] Z. Cheng, Z. Pang, Y. Liu, and P. Xue, "An adaptive solar photovoltaic array reconfiguration method based on fuzzy control," in *Proc. 8th World Congr. Intell. Control Autom.*, 2010, pp. 176–181.

[14] G. Carannante, C. Fraddanno, M. Pagano, and L. Piegari, "Experimental performance of MPPT algorithm for photovoltaic sources subject to inhomogeneous insolation," *IEEE Trans. Ind. Electron.*, vol. 56, no. 11, pp. 4374–4380, Nov. 2009.

[15] E. V. Paraskevadaki and S. A. Papathanassiou, "Evaluation of MPP voltage and power of mc-Si PV modules in partial shading conditions," *IEEE Trans. Energy Convers.*, vol. 26, no. 3, pp. 923–932, Sep. 2011.
[16] H. Patel and V. Agarwal, "Maximum power point tracking scheme for PV systems operating under partially shaded conditions," *IEEE Trans. Ind. Electron.*, vol. 55, no. 4, pp. 1689–1698, Apr. 2008.
[17] M. Lei, S. Yaojie, L. Yandan, B. Zhifeng, T. Liqin, and S. Jieqiong, "A high performance MPPT control method," in *Proc. Int. Conf. Mater. Renewable Energy Environ.*, 2011, vol. 1, pp. 195–199.
[18] S. Kazmi, H. Goto, O. Ichinokura, and H.-J. Guo, "An improved and very efficient MPPT controller for PV systems subjected to rapidly varying atmospheric conditions and partial shading," in *Proc. Australasian Univ. Power Eng. Conf.*, 2009, pp. 1–6.
[19] P. Lei, Y. Li, and J. E. Seem, "Sequential ESC-based global MPPT control for photovoltaic array with variable shading," *IEEE Trans. Sustainable Energy*, vol. 2, no. 3, pp. 348–358, Jul. 2011.
[20] Y.-H. Ji, D.-Y. Jung, J.-G. Kim, J.-H. Kim, T.-W. Lee, and C.-Y. Won, "A real maximum power point tracking method for mismatching compensation in PV array under partially shaded conditions," *IEEE Trans. Power Electron.*, vol. 26, no. 4, pp. 1001–1009, Apr. 2011.
[21] Syafaruddin, T. Hiyama, and E. Karatepe, "Investigation of ANN performance for tracking the optimum points of PV module under partially shaded conditions," in *Proc. Int. Power Energy Conf.*, 2010, pp. 1186–1191.
[22] R. Ramaprabha, B. Mathur, A. Ravi, and S. Aventhika, "Modified Fibonacci search based MPPT scheme for SPVA under partial shaded conditions," in *Proc. 3rd Int. Conf. Emerging Trends Eng. Technol.*, 2010, pp. 379–384.
[23] M. Miyatake, M. Veerachary, F. Toriumi, N. Fujii, and H. Ko, "Maximum power point tracking of multiple photovoltaic arrays: A PSO approach," *IEEE Trans. Aerosp. Electron. Syst.*, vol. 47, no. 1, pp. 367–380, Jan. 2011.
[24] K. Odagaki, "Practical study on 5.2 MW PV system in Sharp's Kameyama plant," in *Proc. Power Convers. Conf. Nagoya*, 2007, pp. 1212–1216.
[25] H. Taheri, Z. Salam, K. Ishaque, and Syafaruddin, "A novel maximum power point tracking control of photovoltaic system under partial and rapidly fluctuating shadow conditions using differential evolution," in *Proc. IEEE Symp. Ind. Electron. Appl.*, 2010, pp. 82–87.
[26] L. Zhou, Y. Chen, K. Guo, and F. Jia, "New approach for MPPT control of photovoltaic system with mutative-scale dual-carrier chaotic search," *IEEE Trans. Power Electron.*, vol. 26, no. 4, pp. 1038–1048, Apr. 2011.
[27] M. Trova, "Top 5 performers in PHOTON inverter tests," presented at the Photon's 1st PV Inverter Conf., Stuttgart, Germany, Apr. 2010.
[28] T. L. Nguyen and K.-S. Low, "A global maximum power point tracking scheme employing DIRECT search algorithm for photovoltaic systems," *IEEE Trans. Ind. Electron.*, vol. 57, no. 10, pp. 3456–3467, Oct. 2010.
[29] N. Femia, G. Petrone, G. Spagnuolo, and M. Vitelli, "Optimization of perturb and observe maximum power point tracking method," *IEEE Trans. Power Electron.*, vol. 20, no. 4, pp. 963–973, Jul. 2005.
[30] T. Kerekes, R. Teodorescu, P. Rodríguez, G. Vázquez, and E. Aldabas, "A new high-efficiency single-phase transformerless PV inverter topology," *IEEE Trans. Ind. Electron.*, vol. 58, no. 1, pp. 184–191, Jan. 2011.
[31] E. Koutroulis and F. Blaabjerg, "Design optimization of grid-connected PV inverters," in *Proc. 26th Annu. IEEE Appl. Power Electron. Conf. Expo.*, 2011, pp. 691–698.
[32] N. Mohan, T. Undeland, and W. Robbins, *Power Electronics: Converters, Applications and Design*, 2nd ed. New York: Wiley, 1995, pp. 164–172.
[33] B. H. Cho, J. R. Lee, and F. C. Y. Lee, "Large-signal stability analysis of spacecraft power processing systems," *IEEE Trans. Power Electron.*, vol. 5, no. 1, pp. 110–116, Jan. 1990.

Eftichios Koutroulis (M'10) was born in Chania, Greece, in 1973. He received the B.Sc. and M.Sc. degrees in electronic and computer engineering and the Ph.D. degree in the area of power electronics and renewable energy sources (RES) from the Technical University of Crete, Chania, in 1996, 1999, and 2002, respectively.

He is currently an Assistant Professor with the Department of Electronic and Computer Engineering, Technical University of Crete. His research interests include power electronics (dc/ac inverters and dc/dc converters), the development of microelectronic energy management systems for RES, and the design of photovoltaic and wind energy conversion systems.

Frede Blaabjerg (F'03) received the M.Sc.EE. and Ph.D. degrees from the Aalborg University, Aalborg East, Denmark, in 1987 and 1995, respectively.

From 1997 to 1998, he was with ABB-Scandia, Randers. During 1988–1992, he was a Ph.D. student with Aalborg University, where he became an Assistant Professor in 1992, an Associate Professor in 1996, a Full Professor in power electronics and drives in 1998, and the Dean of the Faculty of Engineering, Science, and Medicine during 2006–2010. He is currently with the Department of Energy Technology, Aalborg University. He has also been a part-time program Research Leader with Research Center Risoe in wind turbines. In 2009, he became a Visiting Professor with Zhejiang University, Hangzhou, China. His research interests include power electronics and its applications, such as wind turbines, photovoltaic systems, and adjustable-speed drives.

Since 2006, he has been the Editor in Chief of the IEEE TRANSACTIONS ON POWER ELECTRONICS. He was a Distinguished Lecturer for the IEEE Power Electronics Society from 2005 to 2007 and a Distinguished Lecturer for the IEEE Industry Applications Society from 2010 to 2011. In 1995, he received the Angelos Award for his contributions to modulation techniques and the Annual Teacher Prize from Aalborg University. In 1998, he received the Outstanding Young Power Electronics Engineer Award from the IEEE Power Electronics Society. He has received ten IEEE Prize Paper Awards and another Prize Paper Award from Power Electronics and Intelligent Control for Energy Conservation Poland in 2005. He received the IEEE Power Electronics Society Distinguished Service Award in 2009, as well as the European Power Electronics and Drives-Power Electronics and Motion Control Council Award in 2010.